Acoustic Interactions in a Rectangular Cavity with a Forced Vibrating Top Elastic Plate Filled with a Compressible Fluid

Manuel Gascón-Pérez

Escuela Técnica Superior de Ingeniería Aeronáutica y del Espacio
Universidad Politécnica de Madrid
Pza. Cardenal Cisneros, 3
28040 Madrid, Spain
tel 910675737
manuel.gascon@upm.es
orcid.org/0000-0003-4593-730X
Received
Revised
Acoustic cavities are founded in many technological applications such as in naval or aerospace engineering. In this paper the vibroacoustic characteristics of a forced vibrating plate at top position of a rectangular cavity filled with an ideal fluid are studied. The velocity potential function is obtained by the method of separation of variables applied to the corresponding wave equation and the pressure field is deduced from the momentum's linearized equation. After an integration over the surface of the plate of its dynamic motion equation considering the orthogonallity of the functions involved expressed in series expansion of the associated modes, analytical expressions are obtained for the calculus of the plate natural or free frequencies of vibration, and the system frequency response for the case of forced vibration. The frequency response or spectrum of the plate deformation, as well as the sound pressure level at different points of the cavity are obtained, and the influence of various parameters such as container height, fluid density and load position on these spectrums are analyzed. Also the mean quadratic sound pressure level over the plate and the mean quadratic deformation level of the plate in vacuum and with fluid are obtained, and finally the variation of the mean quadratic sensibility with the frequency is calculated. Validation of the method is made by comparing the results with those obtained by other authors and theories.

Keywords top plate of rectangular cavity · fluid-structure interaction · natural frequencies · frequency response forced vibrating plate · compressibility effects · fluid velocity potential.

1 Introduction

Fluid-structure interaction regarding an elastic vibrating plate with an acoustic cavity is encountered in many practical aerospace, naval and civil engineering applications such as, for instance, aircraft and ship cabins, bedrooms, sonar cavities, etc.

The noise generated by these vibrating structures (structure-borne noise) in cavities must be considered due to the influence on the comfort of operator and passengers in the cabins of surface vehicles, aircrafts or ships, that are simplified represented by a cavity structure with a vibrating side wall. So a good comprehension of the fluid-structure interaction regarding a structure and a sound cavity is of critical significance in order to control the sound behaviour on this compartments or cabins and has been analysed since many years ago. High values of the sound pressure level SPL can affect seriously the physiological and mental conditions of the passengers or pilots. Hence care must be taken regarding the vibroacoustic performance of these structures in order to achive a noise reduction characteristic.

Also there are devices used in micro electromechanical systems with similar characteristics of the acoustic cavities, in which is interesting to know the natural frequencies in order to control the performance efficiency and power consumption considering the resonant conditions, such as micropumps, see Laser et al. [1], Pan et al. [2] or Shabani et al. [3], and pressure sensors, see Defay et al. [4].

A vibrating plate of a rectangular container or cavity is a typical modellization of many engineering problems and has been studied since many years ago. Early in 1963 Dowell and Voss [5] studied the effect of a rectangular cavity on panel vibration considering a compressible and inviscid fluid, expanding in a Fourier series the analytic solutions for the structure deformation and fluid pressure. Similarly, Pretlove [6,7] analyzed the free and forced vibrations of a rectangular plate backed by a closed rectangular cavity .

Recently researching is more focused on the active control of the coupled system in relation to room acoustics, see Pan et al. [8], active structural acoustic control of sound radiation, see Qiu et al. [9] and active sound transmission control, see Kim et al. [10]. Among these studies, a characteristic approach is the modal coupling theory where the structural vacuum modes and the acoustic rigid cavity modes are determined previously, and then combined to find the performance of the coupled system, but this approach has limitations and is only suitable for weak coupling, and not the case of strong coupling for example for a thin plate, or small cavity height or heavy fluid, and also the continuity on the interface boundary can not be fulfilled.

For the case of complex geometries of engineering structures, the solution is obtained employing finite element methods as well as boundary element methods. Zienkiewicz and Newton [11], analyzed fluid-structure interaction problems employing a finite element technique for the modellization for the structure and the compressible fluid. Sestieri et al. [12] anlyzed a structural-acoustic coupling in cavities with complex geometries making use of the Helmholtz integral equation formulation. Xie et al. [13] analysed a coupled system of an irregular cavity with an elastic plate and general wall impedances and boundary edge conditions taking into account a variational based method.
Gascón-Pérez [14] analysed the hydro-elastic oscillations of the bottom membrane of a rectangular container by considering the fluid incompressible and inviscid; in [15], the same author analyzed the compressibility effects on the vibration of a plate at an off-center position of a rectangular container filled with fluid, and finally in [16] the acoustic radiation characteristics of a forced vibrating elastic panel are investigated.

The acoustic characteristics of a harmonic exited vibrating top plate of a rectangular cavity filled with a compressible and non-viscous fluid is analyzed in this paper. Considering the wave equation for the fluid velocity potential and the pressure field with the momentum's linearized equation, the dynamic equation of the plate is expressed in a series expansion of the associated modes, and after an integration procedure considering the orthogonality condition of the functions involved, an analytical expression is obtained in an elegant manner for the calculus of the plate natural frequencies of vibration for the case of free vibrations, and the system frequency response for the case of forced vibration. Validation of the method is made by comparing the results with those obtained by other authors and theories.

2 Problem Formulation

The dynamic response of the plate of a rectangular cavity subjected to a forcing load q_0 located at x_0, y_0 position, is governed by the equation , see Wang [17]:

$$D\nabla^4 w(x,y,t)+\rho_m t_h \frac{\partial^2 w}{\partial t^2}=p(x,y,t)+\delta q_0(x,y,t) \tag{2.1}$$

Where $D=\dfrac{E\cdot t_h{}^3}{12\left(1-\nu^2\right)}$ is the flexural rigidity, E is the elasticity modulus of the material, t_h is the plate thickness, ν is the Poisson`s ratio, ρ_m is the material density of the plate and w is the plate deflection in normal direction.

The elastic plate is in contact with a fluid and p is the fluid pressure acting on the plate.

And $\delta q_0(x,y,t)$ is the harmonic excitation force per unit area expressed as a Dirac-delta located at x_0, y_0 position associated to a load q_0 of 1N so that

$$\delta q_0(x,y,t)=\delta\tilde{q}_0(x,y)\cdot e^{i\omega t} \tag{2.2}$$

and

$$q_0 = \iint\limits_{S_p} \delta \tilde{q}_0 \left(x - x_0, y - y_0 \right) dx\, dy \tag{2.3}$$

For a plate placed at a position $z = H$, and with l_x, l_y the side lengths of the plate, being H the cavity total height, see Fig.1.

Considering harmonic motion for both the fluid and the plate, the solutions for the pressure and deformation are expressed as:

$$w(x, y, t) = \tilde{w}(x, y) \cdot e^{i\omega t} \text{ and } p(x, y, z, t) = \tilde{p}(x, y, z) \cdot e^{i\omega t} \tag{2.4}$$

The deflection of the plate which is supposed to be simply supported, when coupled with the fluid, will be expressed as a linear combination of the normal modes of the plate in vacuum:

$$w(x, y, t) = \sum_{m,n} w_m^n(x, y) \cdot \bar{d}_m^n \cdot e^{i\omega_m^n t} \tag{2.5}$$

Where $\bar{d}_m^n$ are the weight coefficients associated to each mode that contribute to the total deformation of the rectangular plate in contact with fluid.

The functions $w_m^n\left(x, y\right)$ for a rectangular plate simply supported along its edges, have the general expression, see Wang [17]:

$$w_m^n(x, y) = sin\left(\frac{m\pi x}{l_x}\right) \cdot sin\left(\frac{n\pi y}{l_y}\right) \tag{2.6}$$

The indexes $m-1, n-1$, represent the number of nodal lines in the y, x directions respectively.
Expanding in series of the deformation modes in vacuum the concentrated load:

$$\delta \tilde{q}_0(x, y) = \sum_m \sum_n \bar{q}_m^n \cdot w_m^n(x, y) \tag{2.7}$$

Where the coefficients have the expression:

$$\bar{q}_m^n = \frac{4}{l_x l_y} \iint\limits_{S_p} \delta \tilde{q}_0 (x - x_0, y - y_0) \cdot w_m^n(x, y) dxdy = \frac{4}{l_x l_y} q_0 \cdot w_m^n(x_0, y_0) \tag{2.8}$$

In Fig.1 the geometrical characteristics of the rectangular cavity are represented, in order to be defined and clarified.

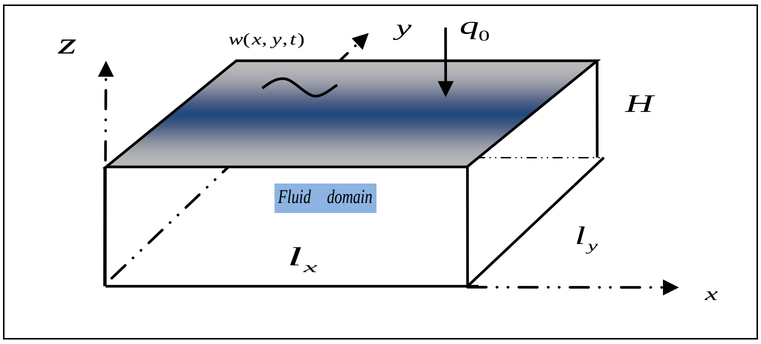

Fig. 1 Scheme of the rectangular cavity with a top plate showing the different geometrical parameters

2.1 Calculus of the Fluid Velocity Potential and Pressure over the Plate

Assuming inviscid fluid and in absence of cavitation, the fluid motion induced by the vibration of the rectangular plate is described using the velocity potential function, Munson [18]. This velocity potential $\varphi(x, y, z, t)$ satisfies the wave equation for the fluid region:

$$\Delta\varphi - \frac{1}{c^2}\frac{\partial^2\varphi}{\partial t^2} = 0 \tag{2.9}$$

And considering harmonic motion $\varphi(x, y, z, t) = \tilde{\varphi}(x, y, z)\cdot e^{i\omega t}$, the Helmholtz`s equation is deduced:

$$\Delta\tilde{\varphi} + k^2\tilde{\varphi} = 0 \tag{2.10}$$

Being k the wave number, $k = \frac{\omega}{c}$, Δ the Laplace operator, and c the sound speed that can be expressed as $c = \frac{B}{\rho_f}$ with B the fluid bulk modulus and ρ_f the fluid density, together with the boundary conditions:

- For the rigid wall boundaries, i.e. the lateral and bottom surfaces of the rectangular cavity $\frac{\partial\varphi}{\partial n} = 0$, being n the normal to the wall surfaces: (2.11)
- For the plate boundary:

$$\frac{\partial\varphi}{\partial z} = \frac{\partial w}{\partial t} \quad \text{for} \quad z = H \quad 0 \le x \le l_x \quad 0 \le y \le l_y \tag{2.12}$$

Applying a method of separation of variables in space-time and expanding in series, the velocity potential function for the fluid domain and the plate deformation are expressed:

$$\varphi(x, y, z, t) = \sum_{m,n}\varphi_m^n(x, y, z)\cdot f_m^n(t) \tag{2.13}$$

$$w(x, y, t) = \sum_{m,n} w_m^n(x, y)\cdot d_m^n(t) \tag{2.14}$$

where for harmonic motion $f_m^n(t) = \overline{f}_m^n \cdot e^{i\omega_m^n t}$ and $d_m^n(t) = \overline{d}_m^n \cdot e^{i\omega_m^n t}$ (2.15)

Considering Eq. (2.9) for the velocity potential and the boundary conditions (2.11), and applying again separation of variables in space coordinates, the solution takes this form:

$$\varphi\ (x, y, z, t) = \sum_{m,n}\varphi_m^n(x, y)\cdot\cosh\left(\lambda_m^n z\right)\cdot f_m^n(t) \tag{2.16}$$

Where the function

$$\varphi_m^n(x, y) = \cos\left(\frac{m\pi x}{l_x}\right)\cdot\cos\left(\frac{n\pi y}{l_y}\right) \tag{2.17}$$

and the parameter

$$\lambda_m^n = \sqrt{\left(\frac{m\pi}{l_x}\right)^2 + \left(\frac{n\pi}{l_y}\right)^2 - k^2} \tag{2.18}$$

Taking into account the boundary condition (2.12) of the fluid-plate interface, the expression for the fluid velocity potential (2.16) and the plate deformation, equation (2.14), and after integration over the plate surface of the squared series expressions involved, the following expressions are obtained:

$$\iint_{S_p}\left(\sum_{m,n}\left(f_m^n\cdot\varphi_m^n(x, y)\cdot\lambda_m^n\cdot\sinh\left(\lambda_m^n H\right)\right)\right)^2 dxdy = \iint_{S_p}\left(\sum_{m,n}\left(\dot{d}_m^n\cdot w_m^n(x, y)\right)\right)^2 dxdy \tag{2.19}$$

from where it is deduced:

$$f_m^n(t) = \frac{1}{\lambda_m^n\sinh\left(\lambda_m^n H\right)}\dot{d}_m^n(t) \tag{2.20}$$

To evaluate the fluid pressure field in the fluid domain, neglecting gravity effects and for small displacements, the momentum's linearized equation is deduced, Munson [18]:

$$\frac{\partial \varphi}{\partial t}+\frac{p}{\rho_f}=0 \tag{2.21}$$

Considering the Eq. (2.16) for the velocity potential and Eq. (2.21), the fluid pressure field is deduced for the cavity domain with the fluid density ρ_f :

$$p(x,y,z,t)=-\rho_f \sum_{m,n} \varphi_m^n(x,y)\cdot\cosh\left(\lambda_m^n z\right)\cdot \dot{f}_m^{\,n}(t) \tag{2.22}$$

By substituting (2.20) in (2.22), the fluid pressure over the plate $z=H$ is:

$$p(x,y,t)=-\sum_{m,n}\frac{\rho_f \cot h\left(\lambda_m^n H\right)}{\lambda_m^n}\,\varphi_m^n(x,y)\,\ddot{d}_m^{\,n}(t) \tag{2.23}$$

And considering (2.15) for harmonic motion:

$$p(x,y,t)=\sum_{m,n} P_m^n(x,y)\,\bar{d}_m^{\,n} e^{i\omega_m^n t} \tag{2.24}$$

Being P_m^n , the pressure mode:

$$P_m^n(x,y)=\frac{\rho_f \cot h\left(\lambda_m^n H\right)}{\lambda_m^n}\,\varphi_m^n(x,y)\,\omega_m^{n\,2} \tag{2.25}$$

2.2 Calculus of the Plate Free Frequencies

First, the free frequencies of vibration of the plate are calculated solving Eq. (2.1) without the forcing load. Considering the expressions in the Eqs. (2.5) and (2.24) for the plate deformation and pressure over the plate, this equation is expressed in a series modal expansion as:

$$\sum_{m,n} D\nabla^4 w_m^n\left(x,y\right)d_m^n(t)-\sum_{m,n}\rho_m t_h \omega_m^{n\,2} w_m^n\left(x,y\right)d_m^n(t)=\sum_{m,n}P_m^n(x,y)d_m^n(t) \tag{2.26}$$

Considering Eq. (2.25) for the pressure and (2.4) for the plate deflection mode and taking into account the expression (2.15) for harmonic motion, and after integration over the plate surface of the squared series expressions of the plate equation, it is deduced:

$$\begin{aligned}&\iint_{S_p}\left\{\sum_{m,n}\left(D\left[\left(\frac{m\pi}{a}\right)^2+\left(\frac{n\pi}{b}\right)^2\right]^2-\rho_m t_h \omega_m^{n\,2}\right)\cdot w_m^n\left(x,y\right)\right\}^2 dxdy=\\&\iint_{S_p}\left\{\sum_{m,n}\left(\frac{\rho_f \cot h\left(\lambda_m^n H\right)}{\lambda_m^n}\,\omega_m^{n\,2}\right)\cdot\varphi_m^n(x,y)\right\}^2 dxdy\end{aligned} \tag{2.27}$$

And with the orthogonality properties of the w_m^n and φ_m^n functions in mind, an analytic simple cuadratic formula is deduced to obtain the modal natural frequencies:

$$A_m^n\cdot\omega_m^{n\,4}+B_m^n\cdot\omega_m^{n\,2}+C_m^n=0 \tag{2.28}$$

Where:

$$A_m^n=\left(\rho_m t_h\right)^2-\left(\frac{\rho_f \cot h\left(\lambda_m^n H\right)}{\lambda_m^n}\right)^2 \tag{2.29a}$$

$$B_m^n=-\left(2\rho_m\, t_h D\,\Lambda_m^{n\,4}\right) \tag{2.29b}$$

$$C_m^n = \left(D\,\Lambda_m^{n\,4}\right)^2 \tag{2.29c}$$

With $\Lambda_m^n = \sqrt{\left(\frac{m\pi}{a}\right)^2 + \left(\frac{n\pi}{b}\right)^2}$

An easy iteration procedure due to the fast convergence is employed for finding the roots or solution, because of the dependence of the parameter λ_m^n with the frequency (wave number k), Eq. (2.18).

2.3 Calculus of the Forced Frequency Response of the Plate

Similarly, the frequency response of the plate is calculated solving Eq. (2.1) but now with the forcing load of frequency ω . Considering the expressions in the Eqs. (2.5) , (2.7) and (2.24) for the plate deformation, concentrated forcing load and pressure over the plate, for harmonic motion, this equation is expressed in a series modal expansion as:

$$\sum_{m,n} D\nabla^4 w_m^n\left(x,y\right)\bar{d}_m^n - \sum_{m,n}\rho_m t_h \omega^2 w_m^n\left(x,y\right)\bar{d}_m^n = \sum_{m,n} P_m^n(x,y)\bar{d}_m^n + \sum_{m,n} w_m^n(x,y)\cdot\bar{q}_m^n \tag{2.30}$$

Considering Eq. (2.25) for the pressure and (2.6) for the plate deflection mode, and after integration over the plate surface of the squared series expressions of the plate equation, it is deduced the following equation:

$$\begin{aligned}&\iint_{S_p}\left\{\sum_{m,n}\left(\left(D\left[\left(\frac{m\pi}{a}\right)^2+\left(\frac{n\pi}{b}\right)^2\right]^2-\rho_m t_h\omega^2\right)\cdot\bar{d}_m^n-\bar{q}_m^n\right)\cdot w_m^n\left(x,y\right)\right\}^2 dxdy =\\ &\iint_{S_p}\left\{\sum_{m,n}\frac{\rho_f\,\cot h\left(\lambda_m^n H\right)}{\lambda_m^n}\,\omega^2\cdot\varphi_m^n(x,y)\cdot\bar{d}_m^n\right\}^2 dxdy\end{aligned} \tag{2.31}$$

With the orthogonality properties of the w_m^n and φ_m^n functions in mind, an analytic quadratics expression is obtained relating the deformation and forcing coefficients $\bar{d}_m^n$ and $\bar{q}_m^n$:

$$Y_m^n\cdot\left(\frac{\bar{d}_m^n}{\bar{q}_m^n}\right)^2 + Z_m^n\cdot\left(\frac{\bar{d}_m^n}{\bar{q}_m^n}\right) + 1 = 0 \tag{2.32}$$

And the deformation coefficient is obtained with the frequency transfer function that relates it with the forcing coefficient:

$$\bar{d}_m^n = TF\left(\omega\right)\cdot\bar{q}_m^n \tag{2.33}$$

Where the transfer function is expressed:

$$TF\left(\omega\right) = \frac{-Z_m^n \pm\sqrt{\left(Z_m^n\right)^2 - 4\cdot Y_m^n}}{2\cdot Y_m^n} \tag{2.34}$$

And the coefficients have the expressions:

$$Y_m^n = A_m^n\cdot\omega^4 + B_m^n\cdot\omega^2 + C_m^n \tag{2.35}$$

$$Z_m^n = \frac{1}{\rho_m\, t_h}\left(B_m^n + 2\cdot\omega^2\right) \tag{2.36}$$

3 Results

For the verification of the method, in Table 1, the frequencies $f_{l\,m}^{n}$ (in Hz) of a simply supported rectangular plate at the top of a rectangular cavity filled with an incompressible fluid, are compared with the results of Gascón-Pérez [15] that analyzes the frequencies of the top rectangular plate of a rectangular container filled with fluid, and are the same, and also calculating the change in the natural frequencies with respect to the vacuum case $f_{v\,m}^{n}$. So the validity of this method can be concluded.

Table 1 Natural frequencies (Hz) for the bottom simply supported steel plate (in vacuum and water) for the present method and the work of Gascón-Pérez [15], of side lengths $l_x = 4$ m, $l_y = 5$ m, container height $H = 3$ m and thickness $t_h = 1$ cm

$m\,,n$	f_v	f_l (Gascón-Pérez [15])	f_l (present method)
1 , 2	5.40	1.74	1.74
2 , 1	7.04	2.41	2.41
2 , 2	9.96	3.68	3.68

Also for the verification of the method, in Table 2, the non-dimensional frequency parameters Ω_m^n defined as $\Omega = \sqrt{\dfrac{\rho_m t_h}{D}}\, l_x^{\,2} \cdot \omega$ of a simply supported rectangular plate at the top of a rectangular container filled with an incompressible fluid, are compared with the results of Zhou et al. [19] that analyze the frequencies of the rectangular plate of a rectangular container filled with a fluid, and the results are aproximately the same with slight discrepancy. The plate is made of aluminium and the relation of fluid-plate material densities is $\rho_f \,/\, \rho_m = 0.125$

Table 2 Natural frequency parameters for the simply supported alluminium plate (in vacuum and dense fluid) for the present method and the work of Zhou et al. [19], , of side lengths $l_x = 1$ m, $l_y = 1$ m, container height $H = 1$ m and thickness $t_h = 5$ mm

Modal number	Ω_v	Ω_l (Zhou)	Ω_l (present method)	Relative discrepancy (%)
1	49.35	39.2	40.4	3.06
2	49.35	39.2	40.4	3.06
3	78.96	66.6	67.7	1.65
4	98.70	85.6	86.1	0.56
5	128.30	112.7	114.0	1.15

The next results are obtained for the case of an aluminium rectangular plate of a rectangular cavity filled with a compressible fluid of density $\rho_f = 1.225 \dfrac{\text{kg}}{\text{m}^3}$, and the following reference characteristics are considered:

Side lengths $l_x = 2$ m, $l_y = 1.5$ m, plate thickness $t_h = 1$ mm, container height $H = 1$ m, and material density $\rho_m = 2700\ \dfrac{\text{kg}}{\text{m}^3}$.

Table 3 presents different natural frequencies of the plate regarding the vacuum case and in contact with fluid

Table 3. Free modal frequencies (Hz) of the reference plate in vacuum and with air for the different modes

Modal number	f_v	f_a
1	1.669	1.539
2	3.471	3.279
3	4.872	4.643
4	6.475	6.207
5	6.675	6.403
6	9.679	9.348
7	10.213	9.873
8	10.680	10.332
9	12.015	11.645
10	13.884	13.485

The sound pressure level at an interior point of the rectangular cavity (the reference point is located at $x = 0.25 l_x \quad y = 0.25 l_y \quad z = 0.5 H$) and the deflexion level of a point of the plate (the reference point is located the center position) are expressed in the following Figs. X-Y in logarithmic scale as SPL (dB) and DL (dB), considering an excitation load q_0 of 1N located at point $x_0 = 0.25 l_x$, $y_0 = 0.25 l_y$ and have the expressions:

$$SPL\,(dB) = 20\log\left(\frac{P}{P_{ref}}\right) \quad \text{with} \quad P_{ref} = 10^{-5}\,\text{Pa}$$

$$DL(dB) = 20\log\left(\frac{w}{w_{ref}}\right) \quad \text{with} \quad w_{ref} = 10^{-12}\,\text{m}$$

Figure 2 presents for the reference values of the panel, the variation of the sound pressure level and the delexion level with the frequency. The different peaks correspond to the resonant frequencies and some of them, but not all, correspond to the natural frequencies of vibration of the plate in contact with the fluid, because there are higher value of natural frequencies of the coupled system than resonant peaks in the showed spectrum range. A peak wavy variation of the plate deflexion level with the frequency is observed in the frequency spectrum (0-15 Hz), while for the interval (15-40 Hz) there is an antiresonant peak, and for higher values of the frequency presents again different peaks. The sound pressure level initially presents a peak wavy variation in the range (0–15 Hz) and almost remains constant in the interval (15-40 Hz), and for higher values of the frequency appear again different peaks. These peaks appear in the form of a doublet peak. All the resonant frequencies coincides for the sound pressure level and the plate deflexion level.

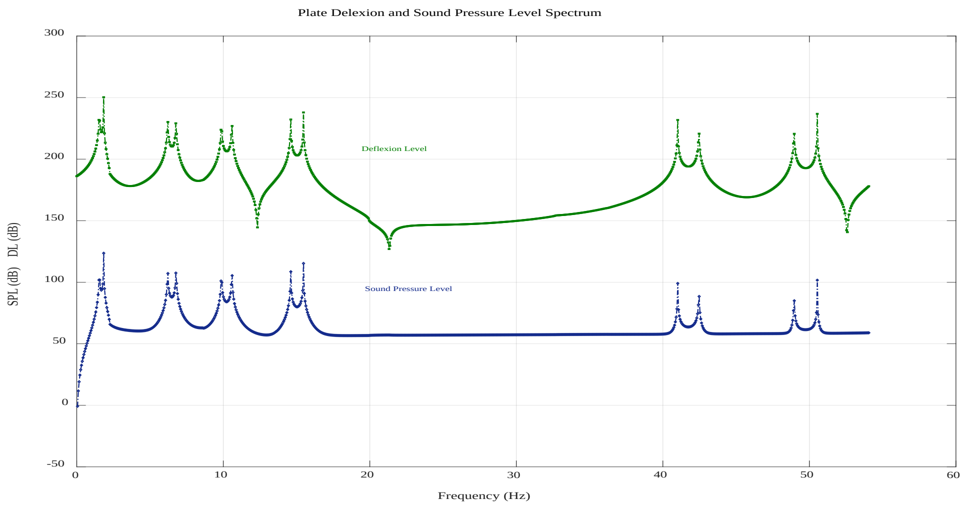

Fig. 2 Variation of the sound pressure Level SPL and plate deflexion level DL with the frequency for the reference conditions.

Figure 3 shows the variation of the sound pressure level SPL with the frequency of the excitation load (located at $x_0 = 0.25 l_x$ and $y_0 = 0.25 l_y$) or the sound pressure level spectrum at a point located at position $x = 0.25 l_x$ $y = 0.25 l_y$ $z = 0.5 H$ of the rectangular cavity, for different values of the fluid density. For the case of heavier fluid the resonant peaks appear at lower values of the frequency and in the form of a single peak (not doublet). Also for heavier fluid appear anti-resonant peaks and not as in the reference case (lighter fluid).

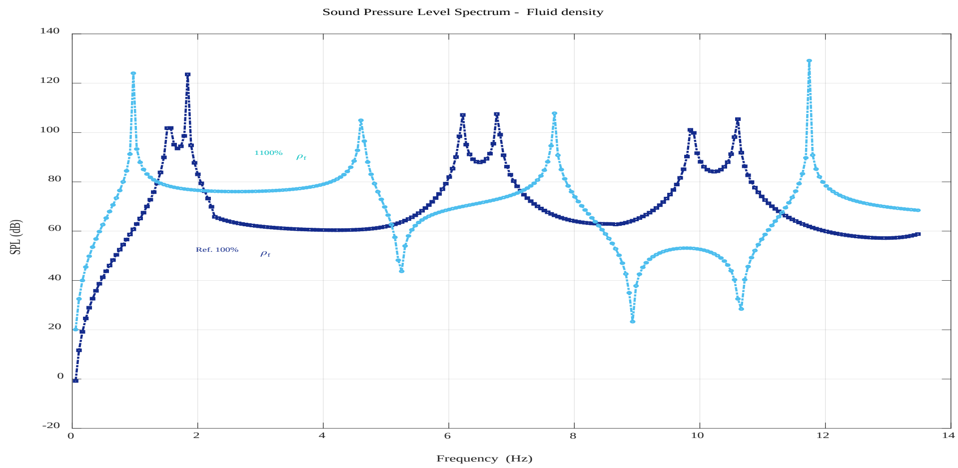

Fig. 3 Variation of the sound pressure level SPL with the frequency for different values of the fluid density

Figure 4 shows the variation of the plate deflexion level DL with the frequency of the excitation load (located at $x_0 = 0.25 l_x$ and $y_0 = 0.25 l_y$) or the plate deflexion level spectrum of the center point of the plate, for different values of the fluid density. For the case of heavier fluid the resonant peaks appear at lower values of the frequency and in the form of a single peak (not doublet). In both cases appear antiresonant peaks. All the resonant frequencies coincides with the corresponding for the sound pressure level of Fig. 3.

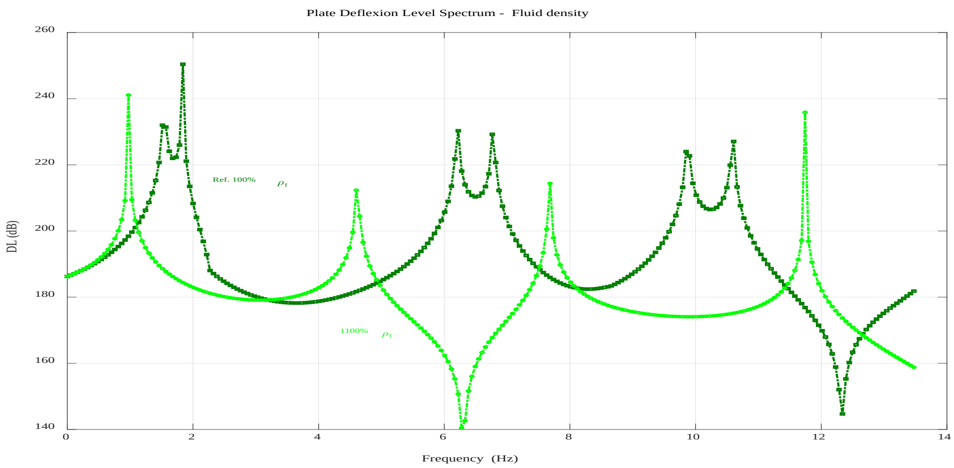

Fig. 4 Variation of the plate deflexion level DL with the frequency for different values of the fluid density

Figure 5 shows the variation of the sound pressure level SPL with the frequency of the excitation load or the sound pressure level spectrum at a point located at position $x = 0.25 l_x$ $y = 0.25 l_y$ $z = 0.5 H$ of the rectangular cavity, for different values of the load position x_0 , y_0 . Some of the resonant peaks for the not-reference position appear at the same frequency that in the reference case, but there are peaks with different frequencies for the two cases. Also there are triplet and quadruplets peaks for the not-reference position. As commented in Fig. 2., some but not all of the peaks have the same frequency than the corresponding natural frequencies of the system. The first resonant peak coincides in frequency for the two load positions.

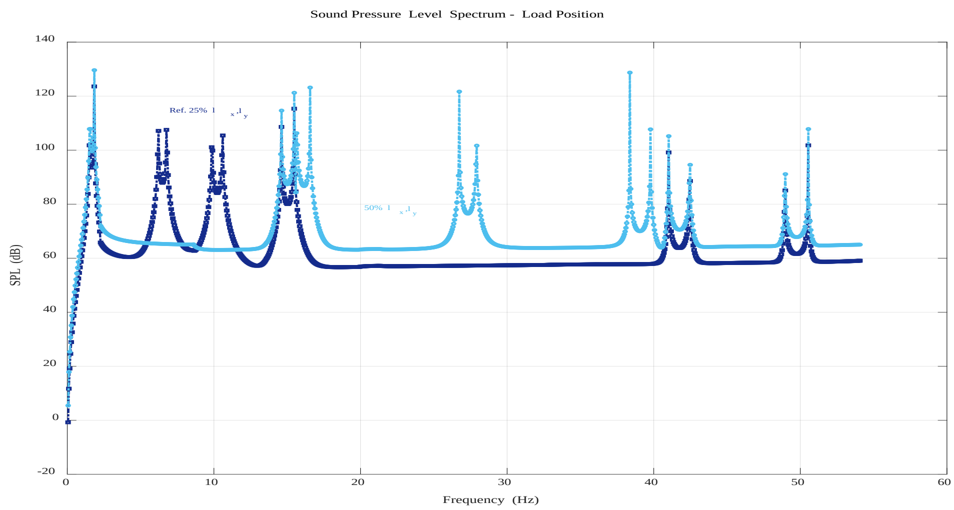

Fig. 5 Variation of the sound pressure level SPL with the frequency for different values of the load position.

Figure 6 shows the variation of the plate deflexion level DL with the frequency of the excitation load with the reference position (located at $x_0 = 0.25 l_x$ and $y_0 = 0.25 l_y$) or the plate deflexion level spectrum of the center point of the plate, for different values of the load position x_0, y_0. The first resonant peak coincides in frequency for the two load positions. For the reference load point position appear some antiresonant peaks, but none in the case of the other load point position. The resonant peaks for the two load positions occur at the same frequency as for the sound pressure level of Fig. 5.

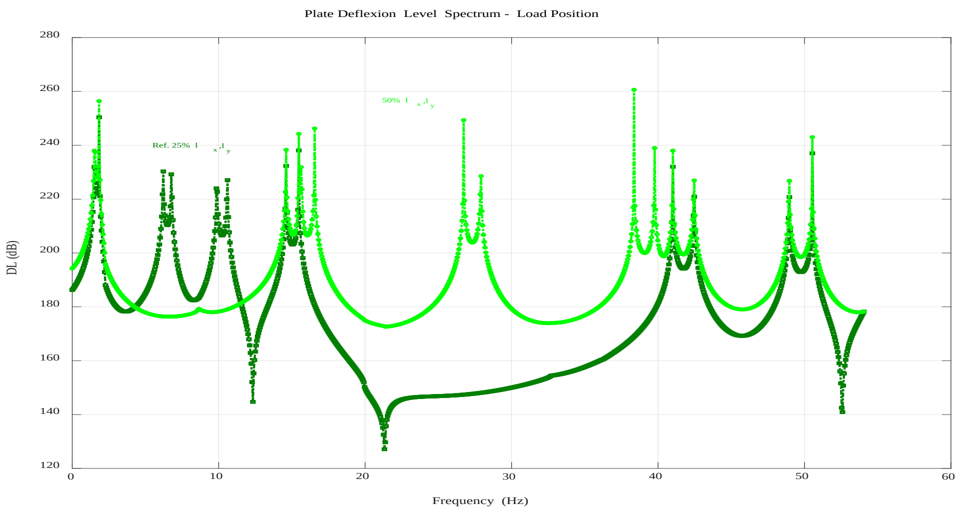

Fig. 6 Variation of the plate deflexion level DL with the frequency for different values of the load position.

Figure 7 shows the variation of the sound pressure level SPL with the frequency of the excitation load (located at $x_0 = 0.25 l_x$ and $y_0 = 0.25 l_y$) or the sound pressure level spectrum at a point located at position $x = 0.25 l_x$ $y = 0.25 l_y$ $z = 0.5 H$ of the rectangular cavity, for different values of the cavity height. For the case of lower height the resonant peaks appear at lower values of the frequency and in the form of a single peak (not doublet). Also for lower height appear an anti-resonant peak and not as in the reference case (higher height).

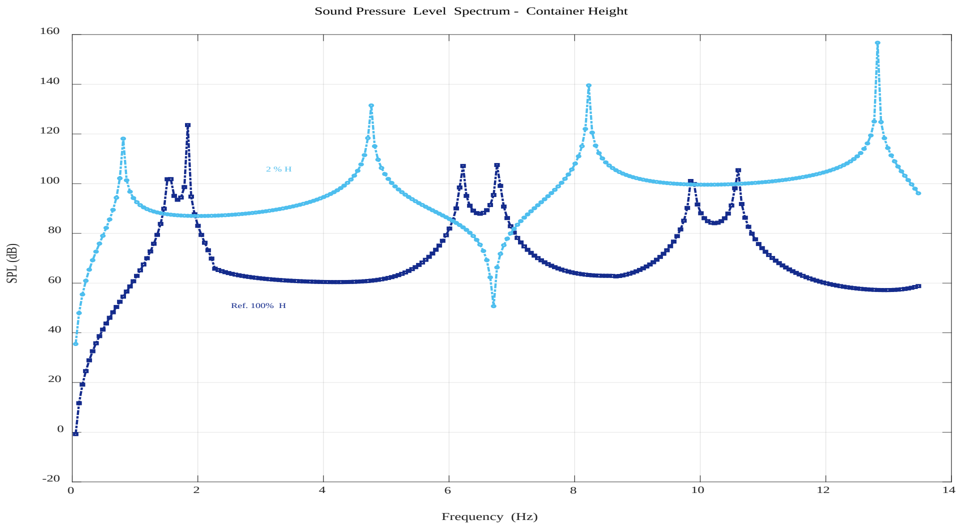

Fig. 7 Variation of the sound pressure level SPL with the frequency for different values of the cavity height.

Figure 8 shows the variation of the plate deflexion level DL with the frequency of the excitation load (located at $x_0 = 0.25 l_x$ and $y_0 = 0.25 l_y$) or the plate deflexion level spectrum of the center point of the plate, for different values of the cavity height. The behaviour is analogous the previous case of Fig. 7. The frequencies of the resonant peaks coincides in the two figures.

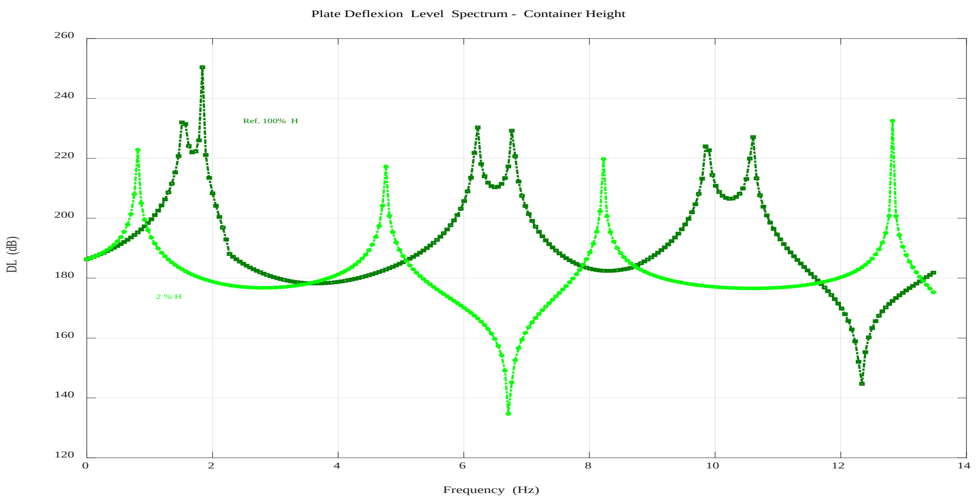

Fig. 8 Variation of the plate deflexion level DL with the frequency for different values of the cavity height.

The frequency spectrum or variation of the sound pressure level SPL and plate deflexion level DL with the frequency, presents no variation with the fluid sound speed c.

Figure 9 shows the variation of the sound pressure level SPL with the frequency of the excitation load (located at $x_0 = 0.25 l_x$ and $y_0 = 0.25 l_y$) or the sound pressure level spectrum at two different points of the rectangular cavity, the reference point located at position $x = 0.25 l_x$ $y = 0.25 l_y$ $z = 0.5 H$ and the point located at position $x = 0.1 l_x$ $y = 0.2 l_y$ $z = 0.5 H$ of the rectangular cavity. This sound pressure level spectrum depends of the location of the fluid point considered inside the cavity. For the new fluid point position appears more resonant peaks, and some of them coincides with the corresponding to the reference case. Many of them, but not all, are coincident with the natural frequencies of the system, so the number of resonant peaks are higher than the natural frequencies of the coupled system.

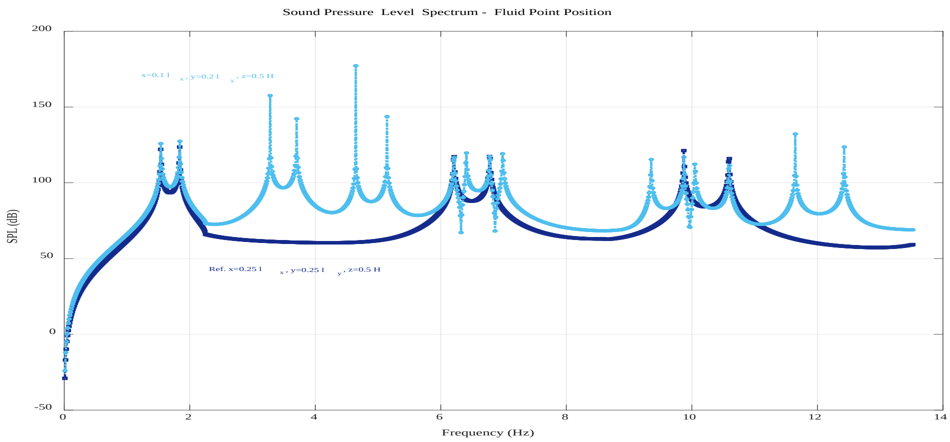

Fig. 9 Variation of the sound pressure level SPL with the frequency for different values of the fluid point position.

Figure 10 shows the variation of the sound plate deflexion level DL with the frequency of the excitation load (located at $x_0 = 0.25 l_x$ and $y_0 = 0.25 l_y$) or the plate deflexion level spectrum at two different points of the rectangular plate, the reference point located at center position $x = 0.5 l_x$ $y = 0.5 l_y$ and the point located at position $x = 0.2 l_x$ $y = 0.3 l_y$ of the rectangular plate. Similarly as in Fig. 9, the frequency response of the plate deflexion depends of the location of the point of the plate considered and the number of resonant peaks is higher for the new plate point position.

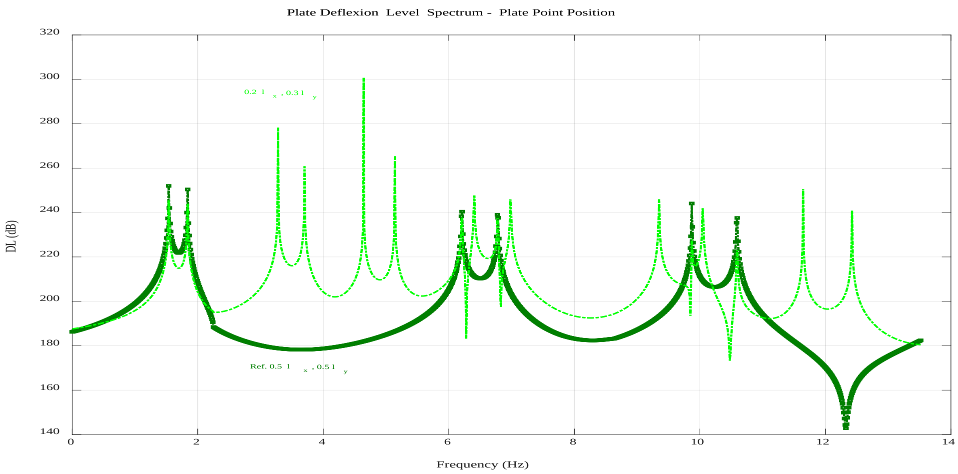

Fig. 10 Variation of the plate deflexion level DL with the frequency for different values of the plate point position.

Figure 11 shows the variation of the mean quadratic plate sound pressure level MQSPL with the frequency of the excitation load (located at $x_0 = 0.25 l_x$ and $y_0 = 0.25 l_y$) or the mean quadratic plate sound pressure level spectrum. There are a lot of resonant peaks, and many of them coincides in frequency with the natural frequencies of the coupled system, but there are more resonant peaks than the number of the natural frequencies of the coupled system. This mean quadratic plate sound pressure level is calculated as:

$$MQSPL\,(dB) = 20\log\left(\frac{MQP}{P_{ref}}\right) \quad \text{with} \quad P_{ref} = 10^{-5}\,\text{Pa}$$

Where MQP is the mean quadratic sound pressure over the plate

$$MQP = \sqrt{\frac{1}{l_x l_y}\iint_{S_p}\left[\sum_{m,n} P_m^n(x,y)\,\bar{d}_m^n\right]^2 dxdy} \tag{2.37}$$

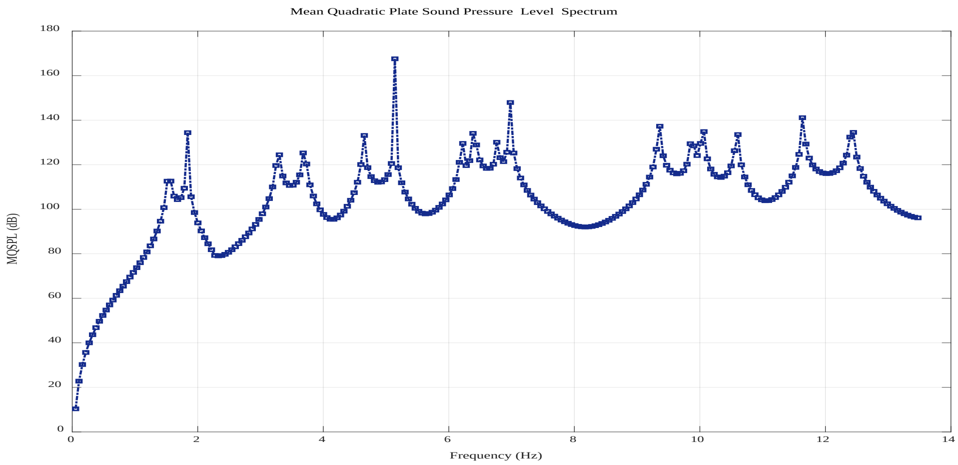

Fig. 11 Variation of the mean quadratic plate sound pressure level MQSPL with the frequency.

Figure 12 shows the variation of the mean quadratic plate deflexion level MQDL with the frequency of the excitation load (located at $x_0 = 0.25 l_x$ and $y_0 = 0.25 l_y$) or the mean quadratic plate deflexion level spectrum. The resonant peaks appear at the same frequency as in the case of Figure 11 for the mean quadratic plate sound pressure. This mean quadratic plate deflexion level is calculated as:

$$MQDL(dB) = 20\log\left(\frac{MQD}{w_{ref}}\right) \quad \text{with} \quad w_{ref} = 10^{-12}\,\text{m}$$

Where MQD is the Mean Quadratic Deflexion of the plate.

$$MQD = \sqrt{\frac{1}{l_x l_y}\iint_{S_p}\left[\sum_{m,n} w_m^n(x,y)\,\bar{d}_m^n\right]^2 dxdy} \tag{2.38}$$

Many of the peak frequencies correspond to the natural frequencies of the plate in contact with fluid inside the rectangular cavity, but there are more peak frequencies than the natural frequencies of the coupled system.

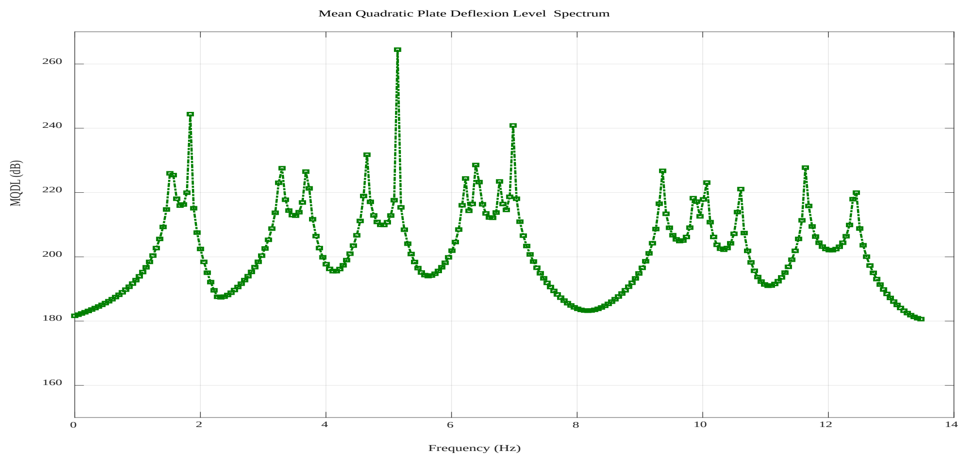

Fig. 12 Variation of the mean quadratic plate deflexion level MQDL with the frequency.

Figure 13 shows the variation of the mean quadratic plate deflexion level MQDL in vacuum with the frequency of the excitation load (located at $x_0 = 0.25 l_x$ and $y_0 = 0.25 l_y$) or the mean quadratic plate deflexion level spectrum. In this vacuum case, the frequencies of the peaks correspond to the natural frequencies of vibration of the plate in vacuum.

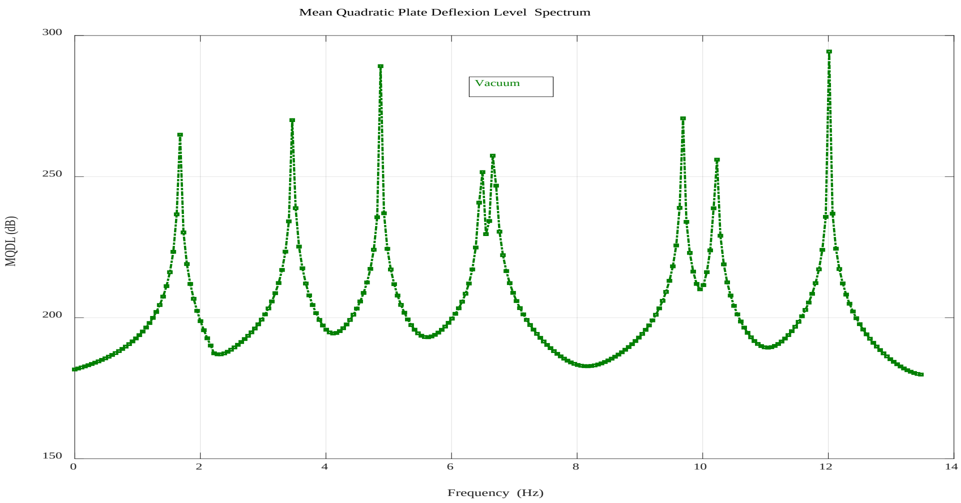

Fig. 13 Variation of the mean quadratic plate deflexion level MQDL in vacuum with the frequency.

Figures 14 and 15 show the variation of the sensibility level SL with the frequency of the excitation load (located at $x_0 = 0.25 l_x$ and $y_0 = 0.25 l_y$) or the sensibility level spectrum for different range of the frequency spectrum. This sensibility level is calculated as:

$$SL(dB) = 20 \log\left(\frac{MQS}{S_{ref}}\right) \quad \text{with} \quad S_{ref} = 10^{-7} \frac{\mathrm{m}}{\mathrm{Pa}}$$

Where MQS is the mean quadratic sensibility of the plate defined as $MQS = \frac{MQD}{MQP}$.

The sensibility decrease with the frequency in the range excitation in the range (0-14 Hz) and the higher values correspond to the low frequency spectrum. In Fig. 15 for a wider range spectrum it can be seen a wavy variation in the range (15-35 Hz) and a decreasing tendency for higher values of the frequency. This is an interesting result for the design of pressure sensors based on the vibration of a plate or diaphragm in an air cavity because the higher values of the sensitivity occur at lower frequencies of excitation of these micro electromechanical systems MEMS.

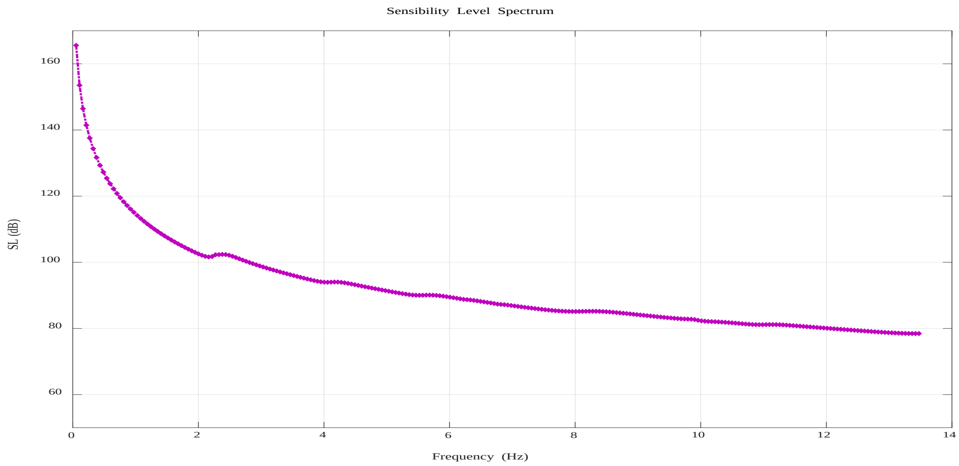

Fig. 14 Variation of the sensibility sevel SL with the frequency (0-14 Hz).

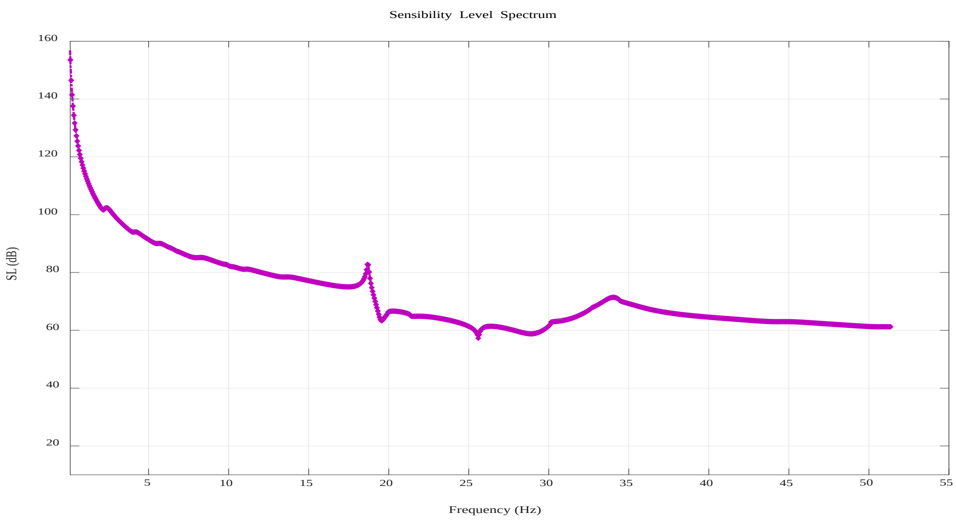

Fig. 15 Variation of the sensibility level SL with the frequency (0, 50 Hz)

4 Conclusions

Acoustic interaction of a vibrating structure with fluid in an acoustic cavity has been studied for the case of a forced excited plate at the top position of a rectangular container filled with compressible and non-viscous fluid. In this regard, the wave equation for the fluid velocity potential is solved by a method of separation of variables, and the acoustic pressure is deduced from the momentum's linearized equation, so that considering the equation of motion of the forced vibrating and after an integration procedure over its surface considering the orthogonallity of the modes involved expressed in series expansion of the associated velocity potential and plate deformation, a simple analytical expressions in an elegant manner is obtained for the calculus of the free or natural vibration frequencies, and the system frequency response for the case of forced vibrating plate of the coupled system. The frequency response or spectrum of the plate deformation of the middle point of the plate expressed in logarithmic scale (dB) as a deformation level and well as the sound pressure level at a point inside the cavity is obtained considering its variation with different parameters such as the container height, fluid density and forced excitation load position. Also is studied the SPL spectrum for different fluid point of the acoustic cavity and the plate deformation spectrum DL for a different plate point position. Furthermore the variation of the mean quadratic plate sound pressure level MQSPL with the frequency is analysed as well as the mean quadratic plate deflexion level MQDL spectrum for the case of vacuum and in contact with fluid. Finally the variation of the mean quadratic sensibility MQS with the frequency is obtained. Validation of the method is made by comparing the results with those obtained by other authors and theories.

References

[1] Laser, D.J., Santiago, J.G.: A review of micropumps. Journal of Micromechanics and Microengineering. 14(6), 35–64 (2004)
[2] Pan, L.S., Ng, T.Y., Wu, X.H., et al.: Analysis of Valveless Micropumps with Inertial Effects. Journal of Micromechanics and Microengineering. 13, 390-399 (2003)
[3] Shabani R, Golzar FG, Tariverdilo S, Taraghi H. et al (2013) Hydroelastic vibration of a circular diaphragm in the fluid chamber of a reciprocating micro pump. International Journal of Engineering 27: 643-650. https://doi.org/10.5829/idosi.ije.2014.27.04a.16
[4] Defay E, Millon C, Malhaire C et al (2002) PZT Thin Films Integration for the Realisation of a High Sensitivity Pressure Microsensor Based on a Vibrating Membrane. Sensors and Actuators A 99: 64-67. https://doi.org/10.1016/S0924-4247(01)00883-4
[5] Dowell EH and Voss HM (1963) The effect of a cavity on panel vibration. AIAA Journal, vol. 1, no. 2, pp. 476-477.
[6] Pretlove AJ (1965) Free vibrations of a rectangular panel backed by a closed rectangular cavity by a closed rectangular cavity Journal of Sound and Vibration, vol. 2, no. 3, pp. 197–209.
[7] Pretlove AJ (1966) Forced vibrations of a rectangular panel backed by a closed rectangular cavity Journal of Sound and Vibration, vol. 3, no. 3, pp. 252–261.
[8] Pan J and Bies DA (1990) The effect of fluid-structural coupling on sound waves in an enclosure—Theoretical part. J. Acoust. Soc. Am. 87(2), 691–707.
[9] Qiu XJ, Sha JZ and Yang J (1995) Mechanisms of active control of noise transmission through a panel into a cavity using a point force actuator on the panel J. Sound Vib. 182, 167–170.
[10] Kim SM and Brennan MJ (2000) Active control of harmonic sound transmission into an acoustic enclosure using both structural and acoustic actuators. J. Acoust. Soc. Am. 107, 2523–2534.
[11] Zienkiewicz OC Newton RE (1969) Coupled vibrations of a structure submerged in a compressible fluid. Stuttgart: Proc. International Symposium on Finite Element Techniques:1–9.
[12] Sestieri E Del Vescovo D and Lucibello P (1984) Structural-acoustic coupling in complex shaped Cavities J Sound Vib. 96(2):219–233.
[13] Xie X , Zheng H and Qu Y. (2016) A variational formulation for vibro-acoustic analysis of a panel backed by an irregularly-bounded cavity. J. Sound Vib. 373:147–16
[14] Gascón-Pérez M (2020) Hydro-elastic oscillations of the bottom membrane of a rectangular container filled with fluid. Defect and Diffusion Forum, 399. Trans Tech Publications Ltd, Switzerland, pp 76-86. https://doi.org/10.4028/www.scientific.net/DDF.399.76
[15] Gascón-Pérez M (2023) Compressibility Effects on the Hydroelastic Vibration of a Plate at an Off-center Position of a Rectangular Container Filled with Fluid Engineering Design Applicatons V Advanced Structured Materials 13 (2). Springer Cham
[16] Gascón-Pérez M (2024) Acoustic Radiation Characteristics of a Forced Vibrating Elastic Panel

under Thermal Environments. Journal of Theoretical and Computational Acoustics, 32 (3)
[17] Wang CY, Wang CM (2014) Structural vibration: exact solutions for strings, membranes, beams and plates. CRC Press, Boca Raton FL.
[18] Munson BR, Okiishi TH, Huebsch WW, Rothmayer AP (2013) Fundamentals of fluid mechanics. John Wiley & Sons, Hoboken, NJ.
[19] Zhou D and Cheung YK (2001) Vibrations of elastic bottom plate of a sealed rectangular container fully filled with liquid. International Journal of Structural Stability and Dynamics 1(1), 145-162.